Cement & Concrete Composites 34 (2012) 604–611

Contents lists available at SciVerse ScienceDirect

Cement & Concrete Composites

journal homepage: www.elsevier.com/locate/cemconcomp

Polymer dispersions and their interaction with mortar constituents and ceramic tile surfaces studied by zeta-potential measurements and atomic force microscopy

Josef Kaufmann [a,*], Frank Winnefeld [a], Roger Zurbriggen [b]

[a] Empa, Swiss Federal Laboratories for Materials Science and Technology, Laboratory for Concrete and Construction Chemistry, Duebendorf, Switzerland
[b] Elotex AG, Sempach Station, Switzerland

ARTICLE INFO

Article history:
Received 10 October 2011
Received in revised form 27 January 2012
Accepted 28 January 2012
Available online 8 February 2012

Keywords:
Polymer dispersion
Tile
Mortar
Tile adhesive
Zeta-potential
Atomic force microscopy

ABSTRACT

The interaction between mineral surfaces and organic polymer dispersions with different monomer base and protective colloids as present in tile adhesive mortar systems was investigated by measuring the ζ-potential and by direct observation by atomic force microscopy (AFM). The charge situation of pure mineral powders and pure polymer dispersions as well as their interaction in presence of different cementitious aqueous solutions was studied. The binding of Ca^{++} ions leads to positive ζ-potentials for quartz or ceramic in calcium containing aqueous solutions and acts as a transmitter of attractive forces. However, the adsorption of sulfate ions may disturb such attraction.

The interaction between polymer dispersions and ceramic (polished and original tile) or mica surfaces influenced by the presence of artificial cementitious pore solutions was observed by AFM. A flat index (height/diameter of latex particles in contact with these surfaces) was defined to quantify the polymer–mineral interface affinity. The different flat indices for different polymer–substrate combinations are mainly related to two parameters, the glass transition temperature of the copolymer and the stabilization system (steric versus cationic). Furthermore tapping phase imaging revealed significant heterogeneities in the inner structure of the polymer particles and inhomogeneous distribution at their surface probably related to local variations of the protective colloid, especially polyvinyl alcohol.

1. Introduction

In order to enhance the properties of cementitious tile adhesives, frequently redispersible polymer powders (RPPs) or liquid polymer dispersions are added. RPPs are gained by spray drying of liquid polymer dispersions, and are available to formulate dry mortars. When mixed with water, RPPs redisperse and achieve the original stage of a liquid polymer dispersion. Polymer dispersions are stable colloidal dispersions of polymer latex particles in an aqueous phase. In order to prevent coagulation, these particles are stabilized through anionic or cationic surfactants, non-ionic steric surfactants or protective colloids. When the mortar system dries due to the ongoing hydration or by evaporation, the arising capillary forces exceed the repulsion forces of the surfactants or the protective colloids and the polymer particles start to form a continuous film. Polymer films bear strong tensile forces and improve the cohesion of the mortar as well as the adhesion to the tile.

The usage of larger and fully vitrified ceramic tiles and their outdoor application [1,2] leads to a strong demand for improved mortar systems and hence better understandings of the factors influencing the film formation process [3].

The performance of a tile adhesive mortar system is mainly dependent on the interaction of the polymer with the cement and fine aggregates (quartz sand and powdered limestone) on the one hand and the interaction with the smooth tile surface on the other hand in a highly ionic cement pore solution environment. This study investigates the different polymer–mineral interactions in a cementitious environment with respect to the particle surface charges and the morphology of adsorbed latex particles, by means of ζ-potential and atomic force microscopy.

While the ζ-potential of the powders can be measured without further treatment of the raw materials, the tile surface was artificially increased by grinding the tile to a fine powder.

A direct observation of the small polymer particles in contact with different surfaces is possible by atomic force microscopy (AFM). High resolution measurement of small interaction forces and the possibility to observe the substrates in environmental conditions are some of the advantages. Mostly, AFM techniques are applied for topological image acquisition. However, atomic force microscopy has been recognized as a useful instrument for the assessment of the local mechanical properties of materials also. A continuous analysis of the force curves at constant peak force even

* Corresponding author. Address: Empa, Ueberlandstrasse 129, 8600 Duebendorf, Switzerland. Tel.: +41 5876540953; fax: +41 587654035.
E-mail address: josef.kaufmann@empa.ch (J. Kaufmann).

0958-9465/$ - see front matter © 2012 Elsevier Ltd. All rights reserved.
doi:10.1016/j.cemconcomp.2012.01.012

allows the mapping of the elastic properties [4]. In this study, it is shown that AFM tapping mode and tapping AFM phase imaging can be successfully applied to observe polymer films and film formation at mineral surfaces and to reveal surface and internal structures of latex particles.

2. Experimental

2.1. Materials

Different polymer dispersions and their interaction with minerals typically present in a tile adhesive mortar system were studied. To be able to study the surface properties, especially the charge situation, powders of these minerals were selected or fabricated. The surface area of a typical tile material was increased artificially by grinding, which allowed the measurement of the ζ-potential to characterize the surface potential and its alteration in presence of different kind of ionic solutions. The atomic force microscopy on the other hand required flat substrates. Mica served as atomic flat model system, whereas industrial tile surfaces also were found to possess flat regions with adequately low roughness to be used as substrates. Furthermore, polished (final polishing with diamond powder of fineness ¼ μm) tile surfaces were used in these experiments.

2.1.1. Polymer dispersions

The selection of polymer dispersions was manifold (see Table 1) and is representative for a majority of commercially available redispersible polymer powders, which vary in the monomer basis (acrylates, vinyl acetate, ethylene, vinyl versatate) as well as in the stabilization system. Except for the cationically stabilized polyacrylic ester based dispersion, the stabilization system consisted of polyvinyl alcohol.

In vinyl acetate based dispersions, the ethylene content was increased systematically. As a consequence, different glass transition temperatures (T_g) ranging from −6 °C to 43.5 °C and film formation temperatures (MFTs) ranging from 0 °C to 18 °C were obtained. An increase of the ethylene content (VA → L-EVA → H-EVA) leads to a lower T_g (and MFT). It has to be mentioned that the surface area of the different polymer dispersions, as measured with a Malvern Mastersizer X equipped with a wet cell dispersion unit MSX15, varied significantly. Beside the T_g and the surface charge, the particle size is another important material parameter, which will be considered in this study.

The surface charge at the slip zone as determined by means of ζ-potential measurements (see below) of the different polymer dispersions ranged from moderate negative to highly positive values. Hereby the cationic protective colloid of the polyacrylic ester leads to a highly positive charged system. An increase of the ethylene content leads to a slightly more positive ζ-potential.

2.1.2. Mineral powders

Commercially available dolomite, limestone and quartz were selected as they are used for mortar production. The chemical composition of the used Portland cement (CEM I 52.5 R) is summarized in Table 2. The qualitative phase compositions of all inorganic powders were assessed by X-ray diffraction using a Panalytical X'Pert Pro diffractometer (Cu Kα radiation, X'Celerator detector). Particle density was determined using the pycnometric method according to European Standard EN 196-6. Density and phase composition are given in Table 3.

In addition, a commercially available fully vitrified ceramic tile (type B-Ia according to EN 14411) was grinded by a rotating disk mill and then sieved down to <63 μm. The particle size distribution of all inorganic powders, as measured with the laser diffractometer (Mastersizer X), is given in Fig. 1. The particle size of the tile powder lies between the ones of quartz and cement. The calcium carbonates have a significantly coarser (limestone) or finer (dolomite) particle size distribution.

For some ζ-potential measurement a 50/50 mass-percent blend of cement and tile powder was used in order to study the importance of each phase in a multi-phase system.

2.2. Methods

2.2.1. Zeta-potential

The ζ-potential is the electrokinetic potential in colloidal systems. For a charged particle moving in a solvent, the layer closest to the surface of the charged particle is composed of condensed or absorbed counter ions. The outer boundary of this layer is defined as the Stern layer. The second layer is composed of ions that diffuse with the charged particle. The boundary of this layer is defined as the slipping plane. The zeta-potential (ζ-potential) is the electric potential at the location of the slipping plane. Its strength is defined by the sum of the surface charge + absorbed ions + diffusing ions.

ζ-potential data were collected with the ZetaProbe (Colloidal Dynamics Inc.), which works on the basis of the electro-acoustic method. A high frequency alternating electric field is applied and causes charged particles to oscillate. The motion of the particles generates a sound wave which is recorded and delivers the dynamic mobility of the suspended particles. The software calculates the ζ-potential from the dynamic mobility. All samples were measured in a beaker and stirred (400 rpm) in order to prevent segregation.

Three different test series were studied. First the ζ-potential of the dispersions was determined. For this tests 10 mass% (dry mass)

Table 1
Polymer dispersions and their properties.

Code	Monomer basis	Stabilization system	T_g[a] (°C)	MFT (°C)	Surface area (m^2/g)	ζ-potential (mV)
Polyacrylic ester						
PAE	Polyacrylic ester	Cationic	17.5	11	8.82	+600
Homopolymer						
VA	Vinyl acetate	Polyvinyl alcohol	43.5	18	6.78	−28
Low ethylene EVA						
L-EVA	Ethylene, vinyl acetate	Polyvinyl alcohol	19.5	4	2.71	−21
High ethylene EVA						
H-EVA	Ethylene, vinyl acetate	Polyvinyl alcohol	−6	0	3.80	−14
VA–VV–BA terpolymer						
VV	Vinyl acetate, vinyl versatate, butyl acrylate	Polyvinyl alcohol	20	8	3.56	+5

[a] Midpoint (as derived by DSC).

Table 2
Chemical composition of the used Portland cement (X-ray fluorescence analysis).

	CaO	SiO_2	Al_2O_3	Fe_2O_3	MgO	Na_2O	K_2O	SO_3	LOI[a]	Others
wt.%	64.9	22.7	3.7	1.4	0.8	0.2	0.7	3.2	1.8	0.6

[a] Loss on ignition according to EN 196-2, includes 1.0 wt.% CO_2.

Table 3
Particle density and qualitative phase composition of the powders used.

Material	Density (g/cm^3)	Qualitative phase composition		
		Main component	Minor component	Traces
Tile	2.49	Amorphous, quartz	Feldspar, cristobalite	Mullite
Quartz	2.65	Quartz		Feldspar
Portland cement	3.13	Alite	Belite, aluminate ferrate, anhydrite	Hemihydrate, calcite, quartz, periclase, arcanite, calcium oxide
Limestone	2.71	Calcite	Dolomite	Quartz
Dolomite	2.86	Dolomite	Calcite	Quartz, feldspar

Alite = tricalcium silicate, belite = dicalcium silicate, aluminate = tricalcium aluminate, ferrate = tetracalcium aluminate ferrate (idealized compositions).

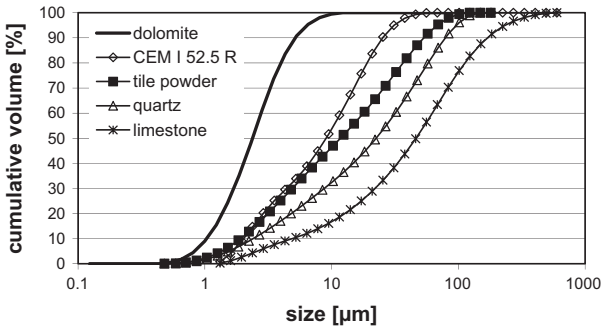

Fig. 1. Particle size distribution of powders.

of the polymer were dissolved in a 0.01 mol/L aqueous NaOH-solution (pH 12.6). The background correction was done with the values as obtained for the 0.01 mol/L aqueous NaOH-solution without added dispersion.

In a second series the ζ-potential of the mineral powders in different aqueous solutions was measured. The selected solutions were distilled water, 1 mol/L KOH, 0.05 mol/L K_2SO_4 and finally a saturated $Ca(OH)_2$ solution. These ions are the most relevant as they represent the most common species in Portland cement pore solutions [5]. The powder content was set to 10 mass%. A measurement point was registered after each minute of powder addition. After the measurement the liquid phase was filtered and used for background correction.

In the third series, titration experiments were performed. The interaction between different polymer concentrations and tile powder or cement was studied. Again, the powder content was set to 10 mass%. Initial sample volume was at 270 mL. Titration was executed at equilibrium conditions in steps of 1 mL of an aqueous (0.01 mol/L NaOH) solution containing 14 mass% (dry mass content) of polymer dispersion, thus the titration steps were at a rate of 0.5 mass% of polymer dispersion per mineral powder mass.

2.2.2. Atomic force microscopy

Generally, in the atomic force microscope (AFM) force fields between the probe (tip) and the sample are used to guide the probe above the surface. In contact mode AFM the force level between the probe and the surface is kept constant so that mostly topological images of the scanned surfaces result. In tapping mode, the probe is scanning over the sample surface, while it is vibrated near the resonance frequency of the cantilever at the same time. This allows a very short and soft contact with the surface. The selectable indention depths are in the order of some tenth of nanometers. Primarily topology and phase information is gathered. Phase imaging creates images of the local distribution of the phase of the tapping signal which is a function of the surface forces that the tip experiences. The phase signal hence contains contributions of the elastic modulus as well as the adhesion forces. AFM images were obtained in tapping mode using a Nanoscope IV MultiMode Scanning Probe Microscope (Digital Instruments Inc., Santa Barbara, CA, USA). AFM tips used here were rectangular silicon Type RTESP7 with a nominal spring constant of 40 N m^{-1} (between 20 and 80 N m^{-1} as specified by the manufacturer). Cantilever length was 125 µm and tip's radius of curvature was less than 10 nm.

For image acquisition, in particular for phase analysis, best contrast was obtained with high free initial amplitudes of about 5.5–6.5 V. Excitation of the cantilever was very close to resonance (drive frequency was 245.2 kHz). Amplitudes with constant surface interaction damping (set point) were selected in the range of 3.5–4.5 V. Lower set points led to a stronger contact between probe and sample and, owing to the relatively soft samples, to smeared images.

For sample preparation a droplet of an aqueous polymer dilution (polymer dispersions diluted with Milli-Q water or artificial cement pore solution; polymer content 0.2 mass%) was put on the substrate surface and then evaporated at 20 °C/70%RH (Fig. 2). Similar methods preparation methods were applied by [6,7]. Alternatively spin coating [8] was tested but temperature drop due to rapid evaporation and size selection through the spinning process was thought to be less controllable. The artificial pore solution simulating the typical ionic composition of the cement pore solution after 1 h of hydration [9] was composed as follows: $[K^+]$ = 444 mM/L, $[Na^+]$ = 40 mM/L, $[Ca^{2+}]$ = 10 mM/L, $[OH^-]$ = 104 mM/L, $[SO_4^{2-}]$ = 200 mM/L, pH = 12.8.

For illustration, the situation of a sample after evaporation as it appears in a SEM (FEI field emission ESEM in low vacuum mode, carbon coated – inhibiting charging) is shown in Fig. 3. The dispersion particles are grouped (partly coagulated) on the surface adopting non-spherical shapes. The image also demonstrates the limitations of a SEM-analysis in relation to resolution. However, variations in the grey values of some particles suggest non-uniform density.

3. Results and discussion

3.1. Zeta-potential measurements

3.1.1. Zeta-potential of powders in aqueous solutions

In this study, the ζ-potentials for the powders in the different aqueous solutions yielded stable values after about 20–30 min.

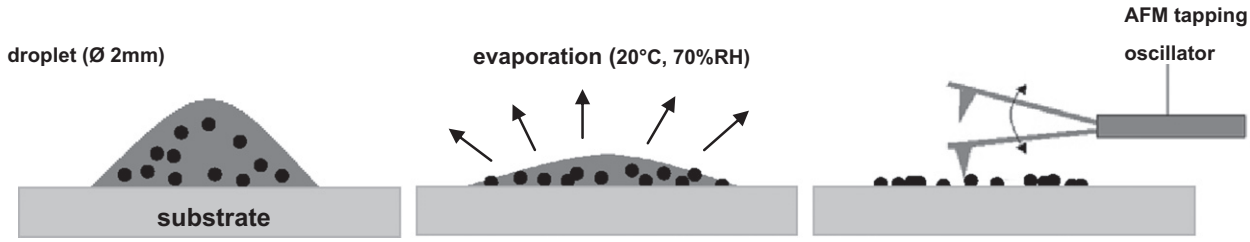

Fig. 2. Placement of a water droplet containing the polymer on a substrate, subsequent evaporation under ambient conditions and final image acquisition by atomic force microscopy in tapping mode (oscillating tip).

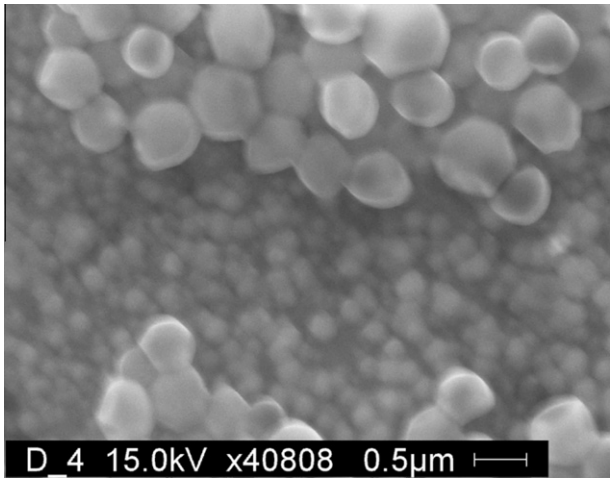

Fig. 3. Low vacuum secondary electron (SE)-image of latex particles of a vinyl acetate homopolymer dispersion (acquired after drying). Note that larger latex particles are on a layer of smaller particles. The latter absorbed onto the surface of a polished tile. Image was done after drying (solvent:water).

The ζ-potentials after 45 min of immersion are plotted in Fig. 4. Owing to the different solutions and selected materials, the pH values are quite different (Table 4). With the exception of water, all powders have the same sign of charge when measured in the same solution; however the absolute values differ significantly. In water, the calcium containing powders induce positive ζ-potentials, while the quartz and the tile lead to negative values, and have almost equal values as when measured in a saturated calcium hydroxide solution. The binding of Ca^{2+} ions leads to the positive ζ-potential

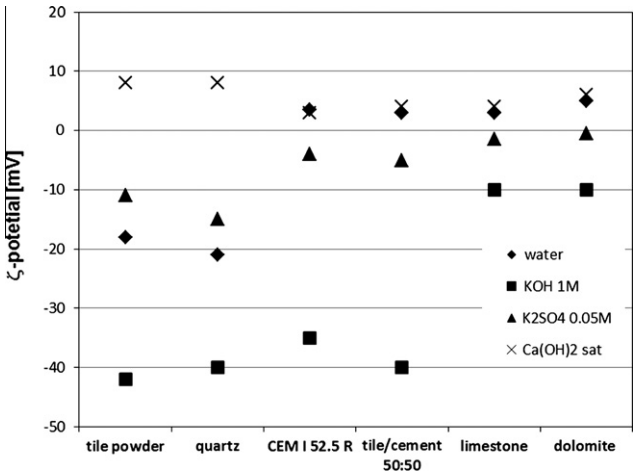

Fig. 4. ζ-potential of inorganic powders in different solutions after 45 min of equilibration.

in these cases. Similar alteration of the ζ-potential was also found for latex dispersions in calcium containing aqueous solutions [10]. Calcium ions hence can act as a transmitter of attractive forces. In a sulfate solution the positive charges provided by the calcium may be overcompensated by negative SO_4^{2-} leading finally to a negative ζ-potential for all powders. However, the absolute values for the calcium containing powders are much lower than for the tile and the quartz powder. The ζ-potential for cement (which also contains calcium) in a KOH-solution is in the range of those of the quartz and the tile powder. Interestingly the dolomite and the calcite are not as sensitive as the other powders to the change of the solution. The tile powder exerts a similar overall behavior as the quartz powder. The ζ-potential of the 50/50 mixture (tile/cement) is dominated by the cement.

No tests were performed on mica, which was used in the atomic force microscopy experiments, but its value was determined in the scope of another study to be in the range of −25 mV in water [11].

3.1.2. Polymer–mineral interaction

The polymer–mineral interaction was studied in the third test series (Fig. 5). With the exception of the polyacrylic ester (PAE), the addition of the different polymer dispersions has relatively little influence on the ζ-potential of the inorganic powders. This is supposed to be due to limited adsorption which may originate in the relatively large size of the polymer particles. The addition of PAE changes the ζ-potential to much more positive values. For the tile powder this even implies a change of sign at the smallest dispersion dosage. Up to a dosage of 1 mass% the ζ-potential increases further and then it decreases between 1 and 3 mass% before it is leveling off at even higher dosages. For the cement suspension, an increase of the ζ-potential with increasing PAE dosage is observed. This behavior can be explained by the cationic protective colloid. In the tile system, the other dispersions show a step in the ζ-potential at a certain dosage. Interestingly the lower the glass transition temperature (T_g) the lower is the critical dosage at which this step occurs (H-EVA → VV → VA). Thus, a lower glass transition temperature seems to facilitate adsorption (this point will be discussed in more details later on).

3.2. Atomic force microscopy

Atomic force microscope tapping mode images of the amplitude and the phase of H-EVA originally dissolved in water or in artificial

Table 4
pH values of solutions with different powders.

	Water	KOH 1 M	K_2SO_4 0.05 M	$Ca(OH)_2$ sat
Tile powder	10.3	14	11.2	12.5
Quartz	8.7	14	7.4	12.6
CEM I 52.5 R	13.1	14	13.4	12.6
Tile/cement 50:50	13.0	14	13.6	12.6
Limestone	9.9	14	10.9	12.6
Dolomite	10.2	14	11.1	12.6

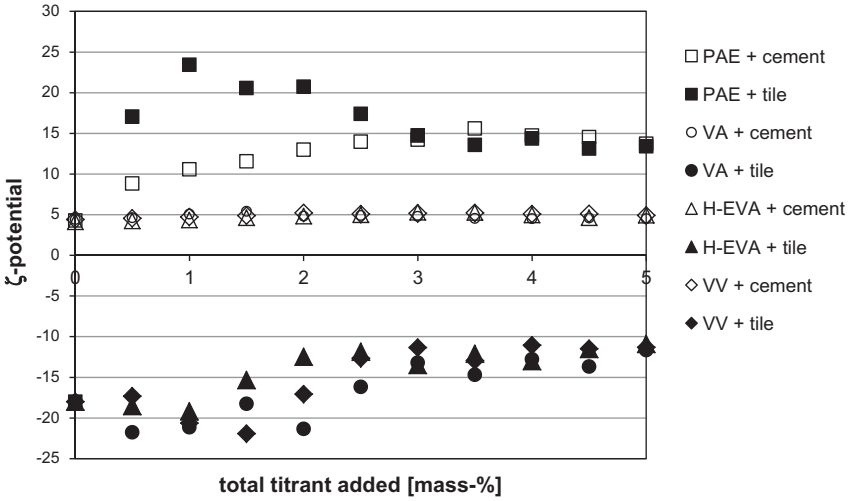

Fig. 5. ζ-potential of different polymer dispersions combined with cement or tile powders.

cementitious pore solution after drying on mica substrates are presented in Fig. 6. In the case of water as a solvent (prior to evaporation) single spheres as well as agglomerated compounds of polymer particles are observed. When the polymer is added to the artificial pore solution prior to evaporation, single spheres are hardly found and film formation is observed. Therefore, the addition of an artificial pore solution seems to facilitate film formation. It has to be mentioned that the artificial pore solution upon drying concentrates and finally precipitation of large crystals was observed which made the selection of AFM image positions difficult. The charge situation might have some influence: The ζ-potential of the tile in presence of the pore solution changes its sign from negative (in pure water) to positive and is hence more attractive for the negatively charged polymer particles.

The phase images clearly allow the distinction of some speckled surface structures (bright). The structures are moderately also present in the topological images (amplitude). Such clear structures are rarely observed in the dried pore solution samples. Applied on polished tile surface, the different polymer dispersions show different film morphologies upon drying (Fig. 7). The process of latex film formation has been divided into three stages: (I) evaporation and ordering, (II) particle deformation which takes place at temperatures above MFT only, and (III) interdiffusion [12]. The process of film formation goes on account of the primary particle morphology. Highest level of film formation (fewest relicts of primary particle structures) is found for PAE, followed by H-EVA. The relatively higher degree of film formation of the PAE with higher T_g and MFT than H-EVA can be explained by the different, cationic protective colloid and the smaller particle size (Table 1) which causes a good affinity to the negatively charged tile surface (in water) and triggers particle coalescence, respectively. Rarely somewhat smaller single particles, which composition unfortunately could

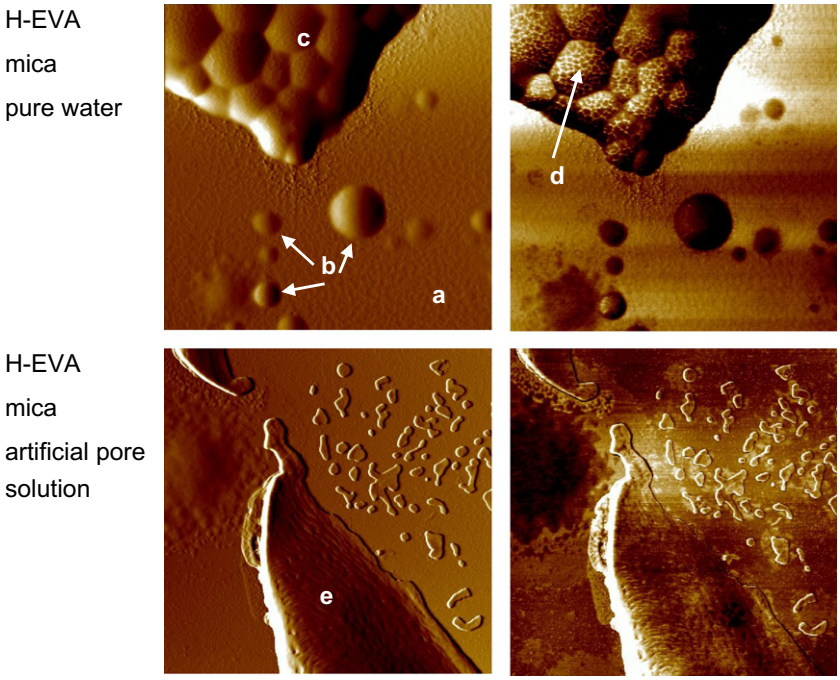

Fig. 6. Amplitude (left) and phase (right) images of H-EVA dissolved in water (top) and artificial pore solution after drying as observed on a mica substrate. Image sizes are 5 μm × 5 μm. (a) Substrate (mica), (b) single polymer particles, (c) accumulated polymer particles, (d) speckled surface structures, and (e) continuous polymer film.

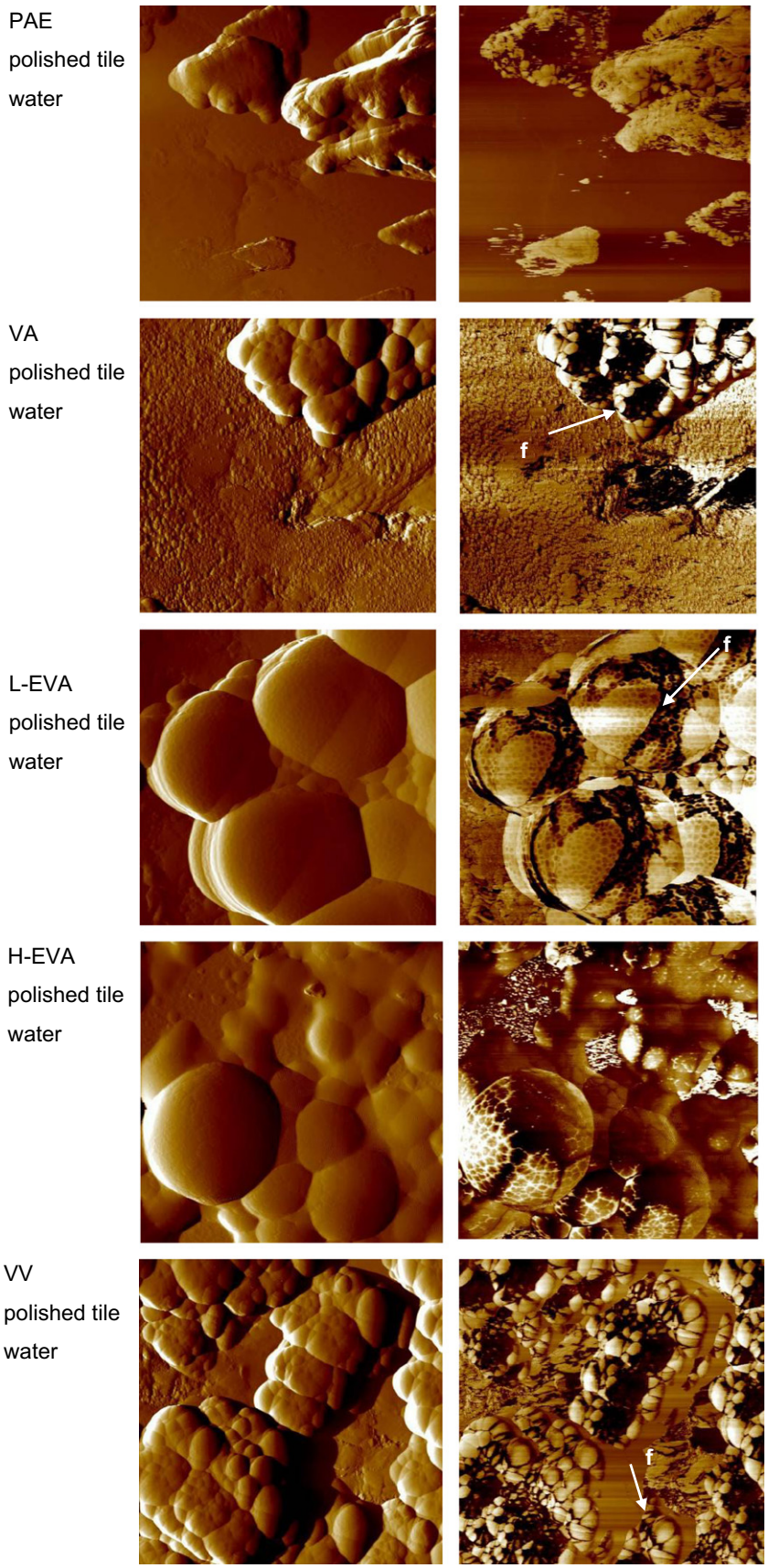

Fig. 7. Amplitude (left) and phase (right) images of different polymer dispersions (dissolved in water) after drying on a polished tile substrate. Image sizes are 5 μm × 5 μm. f: Inner structures of polymer as seen in phase image only.

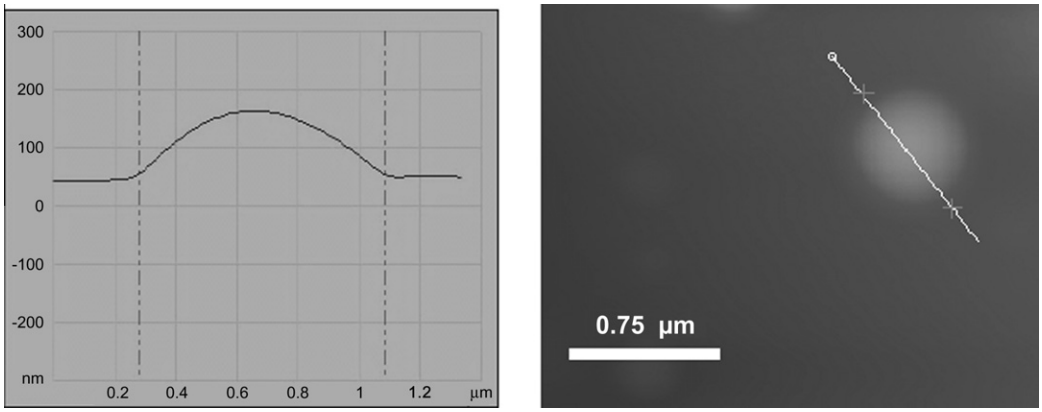

Fig. 8. Determination of diameter and height of single particles (H-EVA, mica, water) from height AFM images.

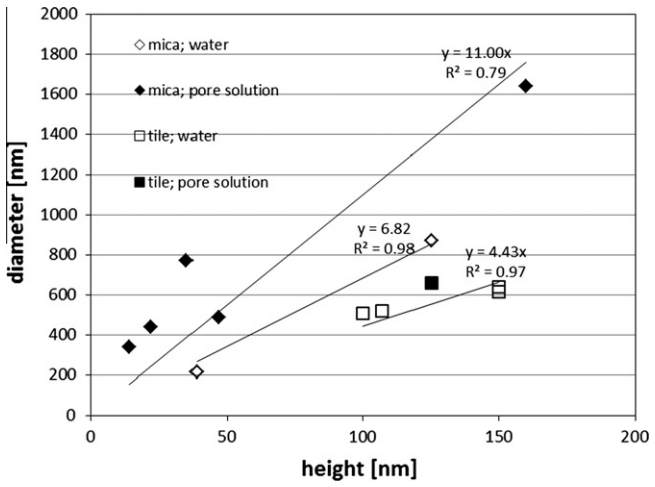

Fig. 9. Regression analysis of diameter versus height of single PAE-latex particles on a polished tile surface. The slope of the regression line (factor of x in regression formula) corresponds to the flat index (=diameter/height).

not be derived, are found. Some structures are repetitive and suggest near-ordering processes. The phase image provides additional information on the composition of the different particle accumulations. For VA, VV and a bit less for L-EVA clearly separable spherical substructures are distinguished indicating a low degree of film formation. Not surprising, these polymers are the ones with slightly higher T_g and MFT temperatures. Furthermore, the phase images reveal superficial speckling and particle substructures such as described in [13]. The large spheres of L-EVA for instance seem to be composed of different smaller particles. The speckling seems to be stronger the higher the ethylene content of the monomer basis is (VA → L-EVA → H-EVA).

A further statistical analysis was performed on the height profiles of the adsorbed latex particles. Single polymer particles were selected and their absolute height and diameter was determined from AFM height images (Fig. 8). Then height versus diameter data was plotted (Fig. 9) and the slope of the linear regression (through 0) was defined as flat index. This index may be used to characterize the substrate–polymer affinity. The larger the diameter compared to the height, the larger the flat index, the larger the affinity of the latex particle to the substrate.

Flat indices as derived for the different polymer dispersions and the different substrates (mica, polished tile, original tile) are plotted versus glass transition temperature T_g and other material parameters in Fig. 10. The pore solution generally leads to a better

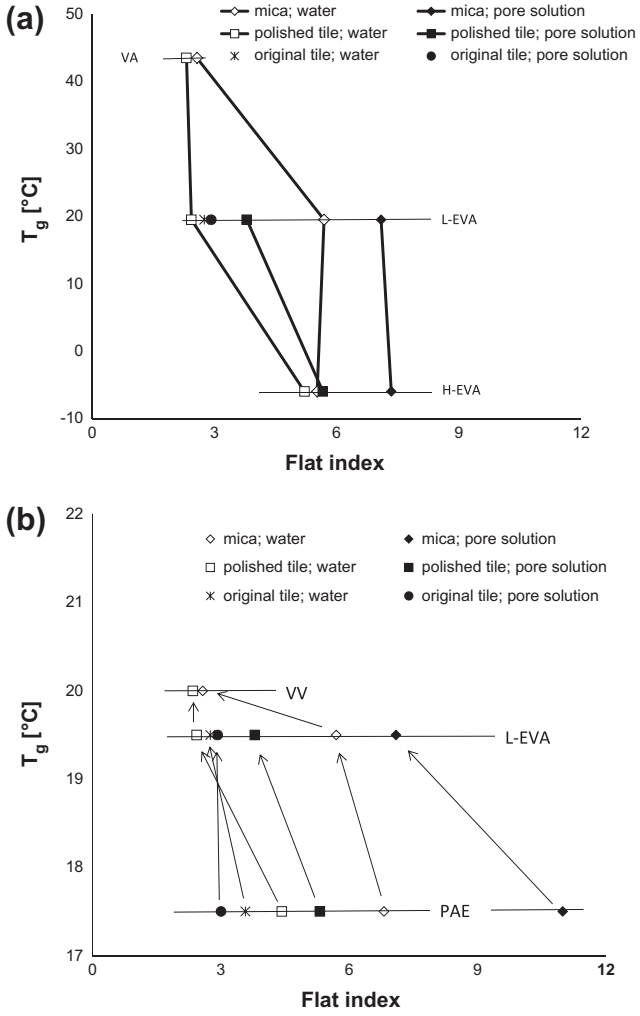

Fig. 10. Flat index (regression d/h) versus T_g of (a) vinyl acetate based polymer dispersions and (b) polymer systems with similar T_g but strongly different stabilization system.

affinity to the substrate (higher flat indices) compared to pure water, especially for the mica. It has a somewhat lower influence for polished tiles and almost no influence is observed on original non-treated tile surfaces. The measurement on original tiles was limited to flat regions at the surface so that a preference of certain mineral composition cannot be excluded despite that EDX-analysis revealed no peculiarities.

In Fig. 10a flat indices of the three polymer systems VA, L-EVA and H-EVA with increasing ethylene content from 0 to about 10 and 20, respectively, are plotted versus their T_g. The higher the ethylene content, the lower the T_g and the higher the flat index. This indicates that an increased deformability of the polymer (given by its lower T_g) increases the ability of a latex particle to change its morphology in order to coat a substrate. Another driving factor for particle deformation and film formation is the particle size. Generally, the smaller a particle, the higher its tendency to film formation in order to reduce its surface energy. However, the fact that the polymer with the highest T_g (VA) and the smallest particle size (highest specific surface, see Table 1) shows the lowest flat indices indicates that the effect of the T_g largely overcompensates the effect of the particle size.

In Fig. 10b the flat indices of three polymer systems with similar T_g are plotted. They strongly differ in the stabilization system (cationically stabilized PAE versus polyvinyl alcohol stabilized VV and L-EVA) and the specific surface. PAE has significantly higher flat indices than VV and L-EVA, because both, the smaller particle size and the cationic stabilization system have a positive effect onto it. But the observation that VV and L-EVA have the same stabilization system but despite of the smaller particle size VV does not have a significant higher flat index, indicates that the particle size has a minor influence on the flat index.

4. Conclusions

The bonding of a tile to a substrate commonly is realized by the application of polymer modified mortars. On the submicron scale, the charge situation at the different interfaces in such a tile polymer–mortar system influences the affinity of the colloidal particles as well as the ability of the polymer dispersions to form films and hence the adhesion and cohesion properties. The charge situation has been studied in different ionic environment by ζ-potential measurements.

Regarding the pure polymer dispersions in water, the ζ-potential is governed by the protective colloid: A cationic polymer leads to a highly positive ζ-potential while a decreasing polyvinyl acetate content lifts the ζ-potential from negative to more positive values.

Regarding the mineral surfaces, the charge situation at a tile surface seems to be similar to the one of a quartz surface resulting in a negative ζ-potential, while the "surface" of the calcium bearing minerals is positively charged so that attractive as well as repelling forces are acting in the system. In the presence of calcium ions, all mineral surfaces give a positive ζ-potential so that these ions can act as bridges to transmit some attractive forces. In presence of sulfate ions their adsorption onto the positive calcium sites may lead to an overall negative ζ-potential. The addition of polymer dispersions to cement or tile surfaces leads to minor changes of the charge situation only. Adsorption at the mineral surfaces seems to be weak.

As observed by atomic force microscopy (AFM), the presence of cementitious ions favors the film formation of polymer dispersions and improves the affinity of the polymer particles to the tile surfaces. The affinity is mostly governed by the glass transition temperature and the stabilization system of the polymer dispersion. A cationic protective colloid seems to facilitate film formation. AFM tapping mode phase imaging revealed details of the inner and the surface structure of the polymer particles and the polymer films. The larger polymer particles seem to be composed of smaller elements with different elastic properties. The polymer surfaces, mainly the ones of polyvinyl alcohol stabilized polymer dispersions, seem to possess substructures introduced by an uneven distribution of the protective colloid. When polymer films are formed such substructures remain, which may influence their adhesion and cohesion properties.

Mortar adhesion strength and shear strength test series, where different polymer systems were measured, indicate that a lower T_g of the polymer can increase the deformability of the mortar at dosages of about 10 mass% [14]. Very often an increased deformability goes on account of a reduced strength. Therefore, with respect to strength properties of a mortar, the T_g, the stabilization system and the particle size of a polymer play only part of the game. In this study we have seen that these polymer parameters can cause a significant improvement on the flat index, which is an indication for the affinity between polymer and mineral substrate. The better the affinity the better adhesion between polymer an mineral substrate is. However, mortar strength is not only dependent on the polymer–mineral interface properties, but also on the cohesion strength of both, the mineral matrix and the polymer films. Therefore, product development must account for both groups of parameters: (i) Polymer–mineral interface parameters, which were investigated in this study, and (ii) phase cohesion parameters as they derive from tensile or shear testing of polymer films, cementitious materials, and real polymer-modified cementitious mortar. Together all data can provide a more comprehensive understanding of adhesion mechanisms of polymer-modified cementitious mortars.

Acknowledgments

The authors would like to thank Markus Ganter (Elotex) for helpful discussions. Financial support by the Swiss Commission for Technology and Innovation (CTI) is gratefully acknowledged (CTI project No. 8605.1 EPRP-IW).

References

[1] Wetzel A, Zurbriggen R, Herwegh M. Spatially resolved evolution of adhesion properties of large porcelain tiles. Cem Concr Compos 2010;32(5):327–38.
[2] Wetzel A, Herwegh M, Zurbriggen R, Winnefeld F. Influence of shrinkage and water transport mechanisms on microstructure and crack formation of tile adhesive mortars. Cem Concr Res 2012;42(1):39–50.
[3] Jenni A, Zurbriggen R, Holzer L, Herwegh M. Changes in microstructures and physical properties of polymer-modified mortars during wet storage. Cem Concr Res 2006;36(1):79–90.
[4] Trtik P, Kaufmann J, Volz U. On the use of peak-force tapping atomic force microscopy for quantification of the local elastic modulus in hardened cement paste. Cem Concr Res 2012;41(1):215–21.
[5] Lothenbach B, Winnefeld F. Thermodynamic modelling of the hydration of Portland cement. Cem Concr Res 2006;36(2):209–26.
[6] Granier V, Sartre A. Ordering and adhesion of latex particles on model inorganic surfaces. Langmuir 1995;11:2179–86.
[7] Engqvist C, Forsberg A, Norgren M, Edlund H, Andreasson B, Karlsson O. Interactions between single latex particles and silica surfaces studied with AFM. Colloid Surf A: Physicochem Eng Aspect 2007;302(1–3):197–203.
[8] Wang Y, Juhué D, Mitchell W, Leung O, Goh C. Atomic force microscopy study of latex film formation. Langmuir 1992;8(3):760–2.
[9] Zingg A, Winnefeld F, Holzer L, Pakusch J, Becker S, Gauckler L. Adsorption of polyelectrolytes and its influence on the rheology, zeta-potential, and microstructure of various cement and hydrate phases. J Colloid Interf Sci 2008;323(2):301–12.
[10] Plank J, Gretz M. Study on the interaction between anionic and cationic latex particles and Portland cement. Colloid Surf A: Physicochem Eng Aspect 2008;330(2–3):227–33.
[11] Ferrari L, Kaufmann J, Winnefeld F, Plank J. Interaction of cement model systems with superplasticizers investigated by atomic force microscopy, zeta-potential, and adsorption measurements. J Colloid Interf Sci 2010;347(1):15–24.
[12] Keddie J. Film formation of latex. Mater Sci Eng Report 1997;21(3):101–70.
[13] Gretz M, Plank J. An ESEM investigation of latex film formation in cement pore solution. Cem Concr Res 2011;41(2):184–90.
[14] Zurbriggen R. Influence of polymer glass transition temperature onto mortar flexibility. In: Russian article in the proceedings of the 6th international scientific and technological conference modern technologies of dry mixtures in building. Moscow, MixBUILD; 2004. p. 67–74.